JOURNAL OF PROPULSION AND POWER
Vol. 16, No. 2, March–April 2000

Experimental Investigation of the Evaporation of Droplets in Axial Acoustic Fields

R. I. Sujith*
Indian Institute of Technology, Madras 600 036, India
G. A. Waldherr†
General Electric Corporate R&D Center, Schenectady, New York 12301
and
J. I. Jagoda‡ and B. T. Zinn§
Georgia Institute of Technology, Atlanta, Georgia 30332

The effect of axial acoustic fields on the evaporation of individual droplets is investigated both experimentally and theoretically. A setup was developed in which images of droplets moving through an acoustic field were acquired using a state-of-the-art, high-speed, intensified video system. The evaporation rates of droplets were determined from the droplet diameters measured from these images. Experimental investigations using methanol droplets showed that the presence of an acoustic field significantly enhances the evaporation of droplets. The evaporation rate is a strong function of the acoustic amplitude, but increases only slightly with frequency. The effect of acoustic oscillations on water and methanol droplet evaporation was theoretically modeled by numerically integrating the differential equations for droplet mass, momentum, and heat transfer. The model uses quasisteady correlations for momentum heat and mass transfer. The model predicted the measured trends correctly. However, the quantitative agreement of these predictions with the experimental data depends strongly on the correlations for Nussult and Sherwood numbers used to model the energy and mass transfer, respectively.

Nomenclature

A = displacement amplitude in Eq. (16), m
B = Spalding number, nondimensional
C_D = drag coefficient, nondimensional
C_P = specific heat at constant pressure, $m^2/s^2/K$
D_{av} = diffusion coefficient, m^2/s
d = droplet diameter, m
k = evaporation constant in Eq. (12), m^2/s
L_V = latent heat of vaporization, J/Kg
l = constant in Eq. (14)
M_A = acceleration modulus, nondimensional
Nu = Nussult number, nondimensional
Pr = Prandtl number, nondimensional
p = pressure, Pa
q = heat transfer per unit area
Re = Reynolds number, nondimensional
r = droplet radius, m
Sc = Schmidt number, nondimensional
Sh = Sherwood number, nondimensional
Sr = Strouhal number, nondimensional
T = temperature, K
t = time, s
U = velocity, m/s
Y = mass fraction, nondimensional
γ = ratio of the droplet density to the air density, nondimensional
Δ_A, Δ_B = empirical constants in Eqs. (7a) and (7b), nondimensional
δ = error
λ = coefficient of thermal conductivity, J/m/s/K
ν = coefficient of kinematic viscosity, m^2/s
ρ = density, kg/m^3
ω = angular frequency, rad/s

Subscripts

a = air
f = final state
l = liquid
p = particle or droplet
R = relative
s = surface
0 = initial state
∞ = freestream

Presented as Paper 95-0485 at the AIAA 33rd Aerospace Sciences Meeting, Reno, NV, 9–12 January 1995; received 4 May 1995; revision received 9 December 1996; accepted for publication 9 February 1999.

*Graduate Student, School of Aerospace Engineering, Georgia Institute of Technology; currently Assistant Professor, Department of Aerospace Engineering.
†Post doctoral Fellow, School of Aerospace Engineering, Georgia Institute of Technology; currently self employed.
‡Professor and Associate Chair, School of Aerospace Engineering, Georgia Institute of Technology.
§Professor and Lewis Chair, School of Aerospace Engineering, Georgia Institute of Technology.

Introduction

THE evaporation of droplets in the presence of acoustic oscillations is an important problem that exists in many engineering applications ranging from liquid-fueled propulsion systems to industrial materials processing. The objective of this investigation is to quantitatively determine the effect of axial acoustic fields on the evaporation of individual droplets.

There is ample evidence in the literature associating acoustic fields with increased convective heat and mass transfer. Results obtained to date have demonstrated that the presence of an acoustic field increases heat and mass transfer to/from stationary objects[1,2] where there is relative motion between the gas phase oscillations and the objects. These findings suggest that acoustic oscillations could increase the rates of transport processes between gases and small particles as long as these particles are not fully entrained by the acoustic field, i.e., when relative motion exists between the two phases. Indeed, additional studies[2–5] have shown that pulsations increase the rates of heat and mass transfer to or from solid spheres or droplets.

The effect of acoustic oscillations on the heat and mass transfer between the gas phase and the fuel spray droplets is of considerable

interest in the field of liquid rocket and ramjet instabilities. In liquid propellant motors, instabilities may temporarily increase the rate of evaporation of the fuel spray, which leads to higher combustion intensities. Any resulting growth in the amplitudes of the oscillations may be detrimental to the performance of the engine and can lead to mission failure. Understanding the effect of acoustic oscillations on spray evaporation is, therefore, essential to develop effective techniques for controlling this type of combustion instabilities in liquid propellant motors. However, to fully understand the effect of pulsations on sprays, it is important to understand their effect on individual droplets.

The possibility that sound or vibrations may increase convective heat and mass transfer in sprays has recently received increased attention, partly due to the prospect of using pulsations to increase the efficiency of a number of energy intensive industrial processes, such as spray drying and calcining. In such processes, the rate controlling mechanisms are the heat and mass transfer between the gas phase and the droplets/particles, which may be enhanced by the presence of pulsations.

The effect of axial acoustic oscillations on droplet motion has been studied and presented elsewhere.[6,7] This paper describes the results of an experimental investigation of the effect of axial acoustic oscillations on the evaporation of individual droplets. An experimental setup was developed in which the rate of evaporation of droplets with and without an acoustic field could be measured. Experiments were performed with methanol droplets. Droplets were injected into a transparent test section in which acoustic oscillations could be excited. The droplets were imaged at two locations in the test section, and the changes in droplet diameters were used to determine the evaporation rates. The experimental results were compared with the predictions from a model that was developed using quasisteady correlations for mass, momentum, and heat transfer.

Experimental Facilities

The facility developed for this study is shown in Fig. 1. It consists of a U-shaped 52-mm-i.d. duct that is closed at one end and open at the other. The entire duct, with the exception of its vertical test section, is made of carbon steel. The test section is 60 cm long and made of Pyrex® to permit optical access from any direction. Droplets can be injected on demand by a piezoelectric droplet generator, installed at the top of the test section.[6] A pair of acoustic drivers fitted to the closed end of the setup are used to excite a standing wave of chosen frequency and amplitude within the tube. Both horizontal steel tubes on either side of the test section are of a trombonelike design that permits their lengths to be changed. The total length of the duct is adjusted until the frequency of the drivers equals that of one of the natural acoustic modes of the pipe. This is necessary to ensure the excitation of resonant, large-amplitude oscillations within the setup. A movable pressure probe was used to measure the axial acoustic pressure distribution along the test section.

The droplet generator produces droplets of constant size while operating in the single-droplet mode. The droplet diameter is a function of the amplitude of the voltage pulse applied to the piezoelectric ceramic transducer, the nozzle diameter, and the volume of any air entrapped in the droplet generator. Small, nonrepeatable amounts of air are always entrapped in the generator when filling it with methanol. Thus, while the diameter of the droplets remained constant throughout a run with a single filling, they could vary slightly when the generator was refilled and operated again.

Droplets were imaged using an intensified, digital, high-speed, charge-coupled device camera. The camera has a resolution of 239 × 192 pixels, and a framing rate of 1000 Hz while acquiring full frame images. A zoom microscope is attached to the camera to obtain sufficient spatial resolution to accurately measure the size of the droplets. The magnification of the camera with the attached zoom lens was calibrated using a reticle. An error of half a pixel can be expected in the droplet diameter measurements. Therefore, the error bars were calculated using the following expression:

$$\Delta = (\pi/2)d_0^2\delta d_0 + (\pi/2)d_f^2\delta d_f = (\pi/4)\left(d_0^2 + d_f^2\right) \qquad (1)$$

where Δ is the error in micrometers per pixel in droplet volume, d_0 is the initial droplet size, d_f is the final droplet size, and δd is the error involved in measuring the droplet diameter.

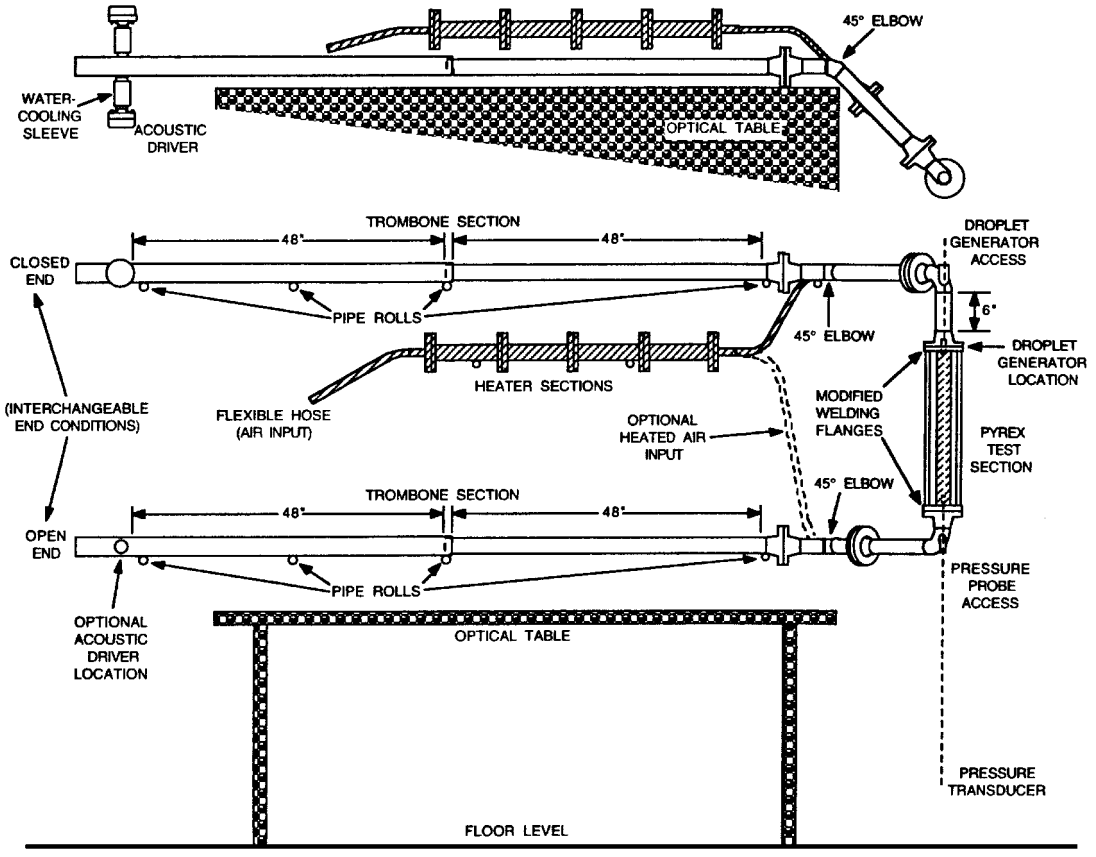

Fig. 1 Schematic of the experimental setup.

It could be argued that the error involved in the diameter measurement is as large as 1 pixel. However, the droplet diameter is determined by fitting a circle around the droplet and not just by determining the coordinates of the extremities of the droplet diameter. The measured diameters are also averaged over many images. Therefore, it is reasonable to assume that the error in diameter measurement is no more than half a pixel.

An expanded, attenuated beam of light from a pulsed copper vapor laser was used as the source of illumination. The laser has an average power of 20 W and can pulse continuously at frequencies ranging from 2 to 10 kHz. The beam is attenuated to approximately 0.5 W using neutral-density filters and is expanded to an area of roughly 2 cm^2 using a system of lenses. The pulses from the laser have a duration of approximately 30 ns, short enough to freeze the droplet motion. The laser frequency was adjusted to be a multiple of the camera frequency using the camera trigger and a frequency multiplier circuit. The camera shutter speed was adjusted to be 10 μs, which is smaller than the period of the laser pulses. This ensured that only one laser pulse illuminates each frame, which result in only one droplet image per frame. Back lighting was used for illumination while acquiring the images. In this technique, a diffuse surface behind the test section is illuminated by the laser. The droplet then appears dark against a bright background, which enhances its visibility.

Experimental Technique

The evaporation of methanol droplets with and without an acoustic field was investigated by imaging the droplets at two locations and comparing their measured diameters. The distance between the two imaging locations was chosen to be an integral multiple of the acoustic half-wavelength to ensure that, for all frequencies, the droplets encountered the same integrated acoustic velocity. All experiments were performed at room temperature.

Droplet sizes ranging from 50 to 150 μm were used in this study. A typical sequence of droplet images is shown in Fig. 2. No droplet deformation is visible. The interdroplet spacing is of the order of 5 cm, which is about 500 times larger than the droplet diameter. Therefore, droplet to droplet flowfield interactions are negligible and do not introduce bias into the measurements. For droplets with diameters larger than 10–20 μm, the mean terminal velocities were too large and the evaporation rates too small to detect significant changes in diameter while the droplets remained within the fixed field of view of the camera. Therefore, the diameter of droplets were measured near the droplet generator and also at a location downstream while the droplet generator was operated in a mode that ejected single droplets of constant diameters.

Droplet images were acquired at the downstream location first. The images were downloaded to a personal computer. The camera was then moved up to the droplet generator, and images were acquired there. The evaporation rate of the droplets were calculated from the mean diameters obtained from the images at these two locations and the distance between them.

Droplet Evaporation Model

A model, very similar to one by Gemmen et al.,[8] has been developed to investigate the effect of acoustics on the evaporation of droplets. However, the acoustic velocity amplitudes for which the computations were performed by Gemmen et al. were 50, 75, and 100 m/s, whereas those encountered in this study were less than 10 m/s. Therefore, calculations corresponding to the conditions in this experiment had to be performed.

The model does not solve the flowfield around the droplet. Therefore, the transport of mass, momentum, and energy between the liquid phase and the gas phase are not solved for directly. Instead, the interactions between the two phases are modeled by using empirical, quasisteady correlations for modeling the drag coefficient, i.e., momentum transfer, Sherwood number, i.e., mass transfer, and Nussult number, i.e., heat transfer. The validity of the quasisteady model is discussed in the results section. Empirical correlations were also used to model the properties of air and liquid.[8,9]

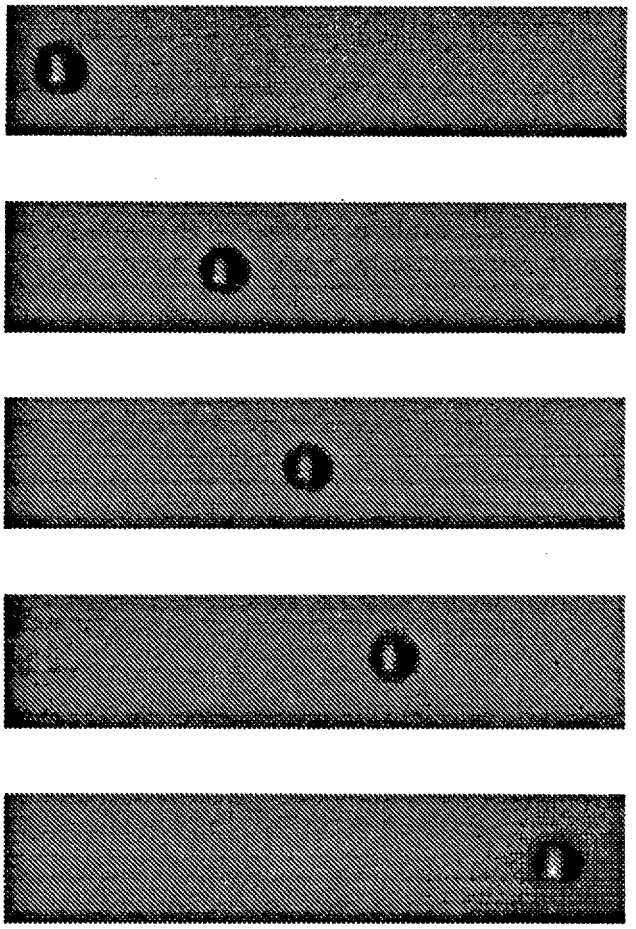

Fig. 2 Typical droplet image sequence.

The development of the model closely follows the experiments described in the earlier section. A droplet was injected into the test section, and calculations of droplet velocity, position, and size were performed for different conditions of temperature, acoustic amplitude, and frequency. The droplets were assumed to be spherical in shape, an assumption that was validated by experimental observations. Internal circulation in the droplet was neglected. The entire droplet was assumed to have uniform properties.

The continuity, momentum, and energy equations were solved simultaneously to determine the evaporation rate of the droplets. This resulted in three ordinary differential equations for the droplet radius, the relative velocity between the droplet and the gas phase, and the droplet temperature, with the initial radius, injection velocity, and the initial droplet temperature as the initial conditions, respectively. The computational procedure is explained next.

The rate of change of the droplet radius can be expressed as[10]

$$\frac{\mathrm{d}r}{\mathrm{d}t} = -\frac{\rho_a}{\rho_l}\frac{D_{\mathrm{av}}}{2r}Sh\,\ell_n(1+B) \tag{2}$$

where ρ_a is the density of air and ρ_l is the density of the liquid. For convective flows, the Sherwood number is a function of Reynolds number Re $(=U_R d/\nu)$ and Schmidt number Sc $(=\nu_a/D_{\mathrm{av}})$. Several empirical correlations that express Sherwood number as a function of Reynolds number and Schmidt number may be found in the literature.[8,10–12] The correlation that is commonly used[8,10,11] is given by the following expression:

$$Sh = 2 + 0.6Re^{\frac{1}{2}}Sc^{\frac{1}{3}} \tag{3a}$$

An alternate correlation for Sherwood number given by Burdukov and Nakaryakov[12] is

$$Sh = 0.37Re^{0.6}Sc^{\frac{1}{3}} \tag{3b}$$

Both the correlations were used in the model in an effort to determine which of the correlations lead to a better prediction of the observed droplet evaporation rates.

B is the Spalding number, which can be expressed as

$$B = \frac{Y_s - Y_\infty}{1 - Y_s} \tag{4}$$

where Y is the mass fraction of the vapor which can be expressed in terms of the partial pressure as

$$Y = \frac{M_v p_v}{M_v p_v + M_a (p - p_v)} \tag{5}$$

where M_v and M_a are the molecular weights of vapor and air, respectively, and p_v is the partial pressure of the vapor. The droplet surface is assumed to be saturated.[13] The saturation partial pressure Y_s of the vapor at the liquid–air interface can be calculated using empirical correlations. The freestream partial pressure Y_∞ is obtained by multiplying the vapor pressure corresponding to the freestream temperature by the relative humidity. The relative humidity was assumed to be zero in these calculations.

The momentum equation of the droplet is given by the following equation[14,15]:

$$\left(\gamma + \frac{\Delta_A}{2}\right)\frac{\mathrm{d}U_R}{\mathrm{d}t} = (\gamma - 1)g - \frac{3C_D U_R |U_R|}{4d}$$

$$- \frac{9\Delta_H}{\mathrm{d}}\sqrt{\frac{\nu}{\pi}}\int_0^t \frac{\dot{U}_R(s)\,\mathrm{d}s}{\sqrt{t - s}} - (\gamma - 1)\frac{\partial U_f}{\partial t} \tag{6}$$

where U_R is the relative velocity, s is the dummy variable used for integration over time, g is the acceleration due to gravity, and U_f is the gas velocity. This equation was derived using the creeping flow assumption ($Re < 0.01$) and then extended to high Reynolds number flows using the empirical constants Δ_A and Δ_H (Ref. 16), which are given by

$$\Delta_A = 2.1 - 0.132\frac{M_A^2}{1 + 0.12M_A^2} \tag{7a}$$

$$\Delta_H = 0.48 + 0.52\frac{M_A^3}{(1 + M_A)^3} \tag{7b}$$

The acceleration modulus M_A is given by the following expression:

$$M_A = \frac{\mathrm{d}}{U_R^2}\frac{\mathrm{d}U_R}{\mathrm{d}t} \tag{7c}$$

A detailed discussion of this equation and its solution using empirical models for C_D is available elsewhere,[14,15] and only a brief outline is given here. The term on the left-hand side of Eq. (6) describes the inertia of the droplet. The first term on the right-hand side corresponds to the gravitational force. The second term is the drag for steady motion corresponding to the instantaneous velocity. The third term allows for the instantaneous drag depending not only on the instantaneous velocities and accelerations but also on the conditions that prevailed during the development of the flow. This is the Basset history integral,[17,18] in which past acceleration is included, weighted as $(t - s)^{1/2}$, where $(t - s)$ is the time elapsed since the past acceleration. The last term is the forcing function due to the acoustic oscillations.

The heat transported to the droplet increases its temperature and supplies the heat of vaporization. The energy equation for the droplet can be written as[10]

$$m_l C_{pl}\frac{\mathrm{d}T_l}{\mathrm{d}t} - 4\pi r^2 \rho_l L_v \frac{\mathrm{d}r}{\mathrm{d}t} = 4\pi r^2 q \tag{8}$$

where q, the heat transfer per unit area to the droplet, is given by

$$q = \frac{\lambda_a (T - T_l)}{2r} Nu \frac{\ell n(1 + B)}{B} \tag{9}$$

For convective flows the Nussult number Nu is a function of Reynolds number Re and Prandtl number $Pr(= \nu_a \rho_a C_p / \lambda_a)$. Several empirical correlations that express Nussult number as a function of Reynolds number and Prandtl number can be found in the literature.[8,10–12] One such correlation that is commonly used is[8,10,11] given by the following expression:

$$Nu = 2 + 0.6Re^{\frac{1}{2}}Pr^{\frac{2}{3}} \tag{10a}$$

An alternate correlation for Nussult number given by Burdukov and Nakaryakov[12] is

$$Nu = 0.37Re^{0.6}Pr^{\frac{1}{3}} \tag{10b}$$

Both the correlations were used in the model in an effort to determine which of the correlations better predicted the observed droplet evaporation rates.

The first term in Eq. (8) describes the energy utilized for heating the droplet. The second term describes the energy used to supply the latent heat of vaporization. The term on the right-hand side describes the heat conducted into the droplet.

The droplet velocity can be written in terms of the droplet displacement as

$$u_P = u_f + u_R = \frac{\mathrm{d}x_P}{\mathrm{d}t} \tag{11}$$

Equations (2), (6), (8), and (11) were integrated using a fourth-order, adaptive Runge–Kutta scheme,[19] with the initial radius, injection velocity, droplet temperature, and the displacement as the initial conditions. The calculations yielded droplet velocity, displacement, diameter, and temperature as functions of time.

Results and Discussion

Preliminary Model Predictions for Water Droplets

The developed model was initially used to predict the evaporation rate of 100–200 μm water droplets at a temperature of 200°C in the absence and presence an acoustic field. The acoustic field consists of a standing wave whose maximum acoustic velocity is 5 m/s. All acoustic velocities mentioned are rms values. The variation of the square of the droplet diameter with time as it evaporates is shown in Fig. 3. The droplet evaporation with and without pulsations approximately follows the D^2 law, i.e.,

$$D^2 = D_0^2 - kt \tag{12}$$

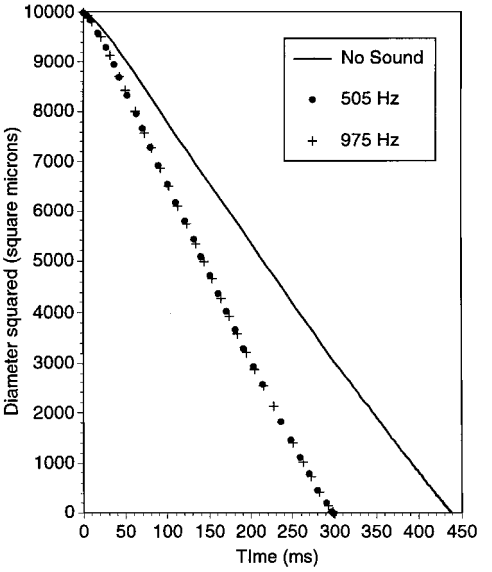

Fig. 3 Theoretically predicted variation of the square of the diameter of a water droplet, initial diameter 100 θm, with time.

In other words, the square of the droplet diameter is linearly dependent on time, both in the absence and presence of an acoustic field.

Figure 3 also shows that the presence of the acoustic oscillations decreases the lifetime of the droplet. The predicted evaporation rate is independent of the acoustic frequency because the quasisteady correlations for the drag, Sherwood number, and Nussult number do not inherently contain any frequency dependence.

The rate of change in droplet diameter due to evaporation at a given rate depends on the droplet diameter itself, as can easily be seen by differentiating Eq. (12),

$$\frac{\mathrm{d}D}{\mathrm{d}t} = -\frac{k}{2D} \tag{13}$$

Therefore, to compare data obtained with different initial droplet sizes, a quantity that does not depend on the initial diameter had to be chosen to quantify evaporation rates, as discussed next.

The droplet terminal velocity is approximately a linear function of the diameter,[6,7,15] i.e.,

$$U_{\text{terminal}} = lD \tag{14}$$

Experiments have shown that the droplets attain their terminal velocity within 5–10 cm from the droplet generator, compared to the 42 cm over which the evaporation rate was measured. Thus, it can be assumed that the droplets fall with terminal velocity throughout the test section. A detailed discussion of the error introduced by this assumption is given in the Appendix.

The droplet displacement x can now be written as

$$x = \int_{t_0}^{t_f} v\,\mathrm{d}t = \int_{D_0}^{D_f} \left(U_{\text{terminal}} \Big/ \frac{\mathrm{d}D}{\mathrm{d}t} \right) \mathrm{d}D$$

$$= \int_{D_0}^{D_f} \frac{lD}{-k/2D}\,\mathrm{d}D = \frac{2l}{3k}\left(D_0^3 - D_f^3\right) \tag{15}$$

It can be seen from Eq. (15) that $(D_0^3 - D_f^3)$ is independent of D_0. Therefore, the volume change of a droplet is independent of the size of the droplet and was chosen to quantify the evaporation rates.

Experimental Data and Comparison with Model Predictions for Methanol Droplets

The following results were obtained using methanol droplets in an unheated test section. The dependence of the volume change of the droplet as it passes through the test section on the magnitude of the acoustic velocity in the standing wave is plotted in Fig. 4 for acoustic frequencies of 410, 820, and 1240 Hz. Figure 4 shows that the measured volume change of the droplets as they traverse the test section increases with acoustic amplitude. Whereas an acoustic field with acoustic velocity amplitude of 5 m/s [corresponding to a sound pressure level (SPL) of 160 dB] increases the evaporation rate of droplets by more than 100%, an acoustic field with acoustic velocity amplitude of 1.6 m/s (corresponding to a SPL of 150 dB) did not enhance the evaporation rate significantly above that in steady flow. The dependence of the droplet volume change on frequency is small, less that the error in the measurements. However, the evaporation rates appear to be generally slightly higher at 1240 Hz than at 410 and 820 Hz.

Also plotted in Fig. 4 are the theoretical predictions obtained from the quasisteady calculations. As mentioned earlier, it was assumed that the droplet temperature is uniform. This amounted to an assumption of infinite thermal conductivity of the liquid phase. This assumption leads to an overprediction of the evaporation rates.

The results obtained using the correlations for the Sherwood and Nussult number given by Eqs. (3a) and (10a), and referred to as theory a in Fig. 4, predicted much higher evaporation rates than were experimentally determined. The results obtained using the correlations provided by Burdukov and Nakoryakov[12] [see Eqs. (3b) and (10b)], and referred to as theory b in Fig. 4, are in better agreement with the experimental data obtained in this study (symbols in Fig. 4), although they still slightly overpredicted the evaporation rates. The theoretical predictions show that, as the acoustic velocity increases from zero, the evaporation rate decreases at first for lower values of acoustic velocity until it reaches a minimum and then increases. This trend could not be experimentally verified because the experimental error was larger than the change in the droplet evaporation rate for small acoustic amplitudes.

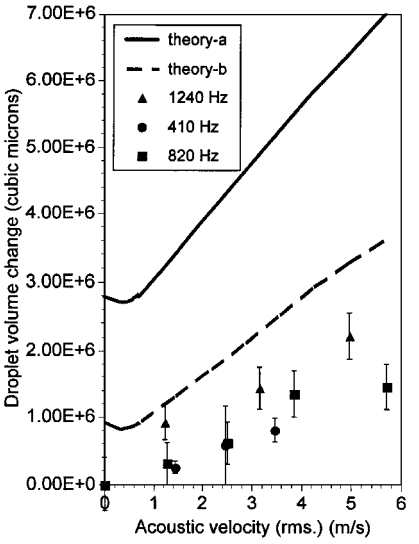

Fig. 4 Change in volume of a methanol droplet moving a fixed distance along a standing wave as a function of acoustic velocity amplitude.

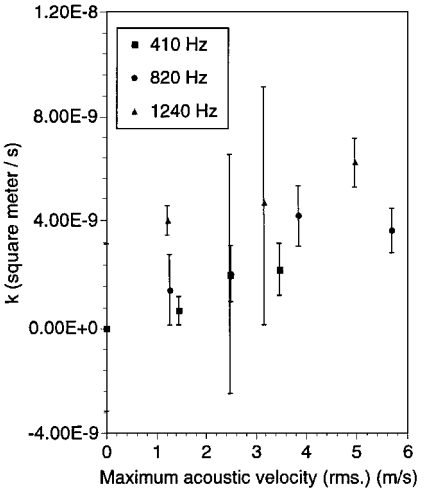

Fig. 5 Dependence of the evaporation constant k on the acoustic velocity amplitude of the standing wave for methanol droplets.

The evaporation constant k for methanol droplets was obtained using the following data reduction procedure. An initial guess of the evaporation constant k was made. The droplet momentum and energy equations, i.e., Eqs. (6) and (8), were integrated with respect to time, with the injection velocity and the initial droplet temperature as the initial conditions. The droplet displacement was calculated by integrating the droplet velocity. The droplet diameter was calculated from Eq. (12), using the measured initial diameter D_0 and the assumed value of k. The integration was continued until the droplet displacement equaled the distance between the camera locations. The value of k was then adjusted until the computed value of the final droplet diameter agreed with its measured value.

The dependence of the evaporation constant on the acoustic velocity is shown in Fig. 5, for frequencies of 410, 820, and 1240 Hz. The evaporation constant clearly increases with increasing acoustic velocity.

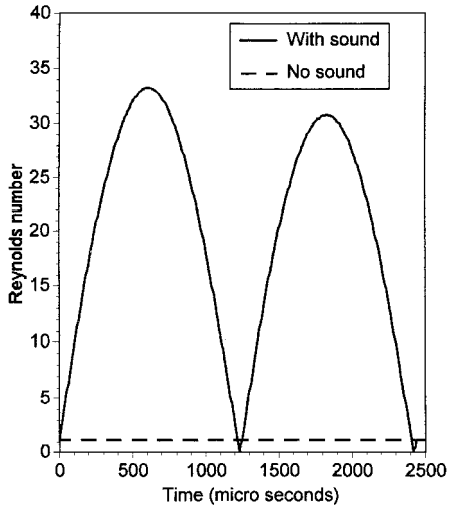

Fig. 6 Variation of Reynolds number based on the relative velocity between the droplet and the gas phase with time as encountered by a droplet moving through one cycle along a standing wave.

The enhancement of evaporation in the presence of an axial acoustic field appears to be due to two reasons: 1) The acoustic field increases the convective heat transfer and mass transfer to and from the droplet, respectively. 2) The presence of an acoustic field decreases the terminal velocity of the droplet, thereby increasing its residence time in the acoustic field.[6,7,20–26] Only the increases in the rates of convective heat transfer and mass transfer are reflected in the increase in k. In other words, k does not account for the increased evaporation due to the increased residence time in the presence of an acoustic field.

An additional explanation for the enhanced evaporation rate of the methanol droplets can be obtained by considering the Reynolds number based on the relative velocity between the droplet and the gas phase. The variation of this Reynolds number with time over one cycle for a 100-μm size droplet in an acoustic field of 410 Hz and velocity amplitude 5 m/s is shown in Fig. 6. Also shown is the Reynolds number for the case of no sound. The presence of acoustic oscillations clearly increase the Reynolds number significantly and, therefore, increases the transport processes, thereby increasing the droplet evaporation rates.

The conditions in this study could be quite different at high ambient temperature and high-pressure conditions in applications such as rocket engines. Under such conditions, droplet deformation and secondary atomization may overshadow the effect of enhanced vaporization reported here. However, the results of this study can directly be applied to industrial processes, such as spray drying, because the conditions encountered there are quite similar to those maintained in this study.

Validity of the Quasisteady Assumption

That the theoretical predictions do not quantitatively match the experimental results brings up the question of the validity of the quasisteady assumption. The mechanisms of mass transfer from spheres under oscillatory flow has been the subject of several investigations. An excellent review of the subject is presented by Al-Taweel and Landau.[3] The mechanism of mass transfer can be modeled by assuming the existance of either a secondary acoustic streaming or a quasisteady state. The choice of the mechanism is usually made on the basis of the ratio between the displacement amplitude of the oscillating flow and the sphere diameter.

Acoustic streaming may be described as the generation of nonzero mean motion by an oscillatory flowfield. The phenomenon typically arises when an acoustic field is attenuated or dissipated, due to its interaction with the medium or with the boundary layer when a solid wall is present. There have been several investigations of acoustic streaming around spheres. A summary of the various investigations are given by Al Taweel and Landau.[3]

To aid the following discussion about the choice of streaming vs quasisteady models, it is useful to introduce a dimensionless frequency parameter, the Strouhal number, which is given by[11,27]

$$Sr = \omega d/\hat{u}_f = d/A \tag{16}$$

where $\hat{u}_f$ is the amplitude of the acoustic velocity and A the displacement amplitude of the oscillating flow. The reciprocal of the Strouhal number, usually referred to in the literature as the A/d ratio, is the ratio between the oscillatory flow displacement amplitude and the diameter of the sphere. This quantity physically represents the distance through which the flow is swept across the surface of a sphere.

At large A/d ratios, heat and mass transfer from the sphere are dominated by the oscillatory velocity component and can be predicted by assuming that, at any instant, steady-state conditions corresponding to the instantaneous velocity are achieved, i.e., a quasisteady analysis can be applied. For lower values of the A/d ratio, the heat and mass transfer processes are dominated by a secondary streaming flow around the droplet, induced by the acoustic field.

The experimental results summarized by Al-Taweel and Landau[3] indicate that, in the absence of mean flow, the transition from conditions where the heat and mass transfer are largely controlled by acoustic streaming to conditions where quasisteady state prevails occurs at a critical A/d of around 0.75. To provide a physical explanation for this, Al-Taweel and Landau suggest that, because it has been shown that in an accelerating flow the sphere must traverse a certain distance before the wake separates, it is possible to suppress separation by reversing the flow within a short interval of time. This would be the case for small A/d ratios in an oscillating flow. As A/d is increased, however, separation can no longer be suppressed, and a quasisteady state can then be assumed to exist. This theory is supported by cited experimental results for cylinders in an oscillating flow, which show that wake separation does not occur for $A/d < 0.637$. No such values for spheres have been reported, but they may be assumed to be roughly of the same order as that for the analogous cylinder.

In most practical applications, however, steady flow is superimposed on oscillations, as is the case of a droplet falling at its terminal velocity. For this case, no clear answer as to when heat and mass transfer by acoustic streaming transitions to quasi-steady-state heat and mass transfer is available in the literature. Reexamining the physical explanation of Al-Taweel and Landau,[3] it can be speculated that in the presence of a steady flow, the probability of wake separation is enhanced for values of A/d much lower than the earlier reported transition value of 0.75 because the flow traverses a greater distance across the sphere. This suggests that a quasisteady state is likely to exist in superimposed steady and oscillating flows, at A/d below the critical value for the no mean flow case.

The droplet diameters used in the study were less than 200 μm, and the maximum frequency was 1240 Hz. Under these conditions, an acoustic velocity higher than 1.46 m/s will satisfy this condition that A/d is larger than 0.75. Therefore, the quasisteady analysis should be able to predict the results. However, the accuracy of the results depends on the validity of the correlations used. It is, therefore, speculated that the reason for the disagreement between the theoretical predictions and the experimental results is due to the inadequacy of the correlations for Sherwood and Nussult numbers rather than a breakdown of the quasisteady assumption.

Conclusions

The effect of acoustic oscillations on the evaporation of droplets was investigated both experimentally and theoretically. Experiments were performed using methanol droplets at room temperature. The data show that the evaporation rate increases with increase in acoustic velocity and with frequency, although the latter dependence is weak. The presence of an acoustic field with a maximum acoustic velocity of 5 m/s (corresponding to a SPL of 160 dB) increases the evaporation rate of droplets by more than 100%, whereas an acoustic field with a maximum acoustic velocity 1.6 m/s (corresponding to a SPL of 150 dB) did not alter the evaporation rate significantly.

The enhancement of the evaporation rate appears to be due to 1) the increase in convective heat transfer and mass transfer to and from the droplet, respectively, caused by the acoustic oscillations and 2) the decrease in the droplet terminal velocity caused by the acoustic oscillations, thereby increasing its residence time in the acoustic field.

The experimental results were compared with the predictions obtained from a model for droplet evaporation that uses empirical, quasisteady correlations for the transport of mass, momentum, and energy. The model predicted the correct trends. The quantitative agreement of the predictions with the experimental data depended on the correlations used for Nussult and Sherwood numbers used to model the heat and mass transfer, respectively. The predictions using the correlation by Burdukov and Nakaryakov were in better agreement with the experimental data than the more popularly used correlations.

Appendix: Independence of the Droplet Volume Change on the Initial Diameter

While proving that the droplet volume change is independent of the initial droplet diameter, it was assumed that the droplets are falling at their terminal velocity and that the terminal velocity is linearly dependent on the diameter. However, the droplets are not injected at their terminal velocity, and they travel some distance before reaching their terminal velocity. Furthermore, the terminal velocity is not exactly linearly dependent on droplet diameter. These deviations from the utilized assumptions can make the droplet volume change a weak function of its initial diameter. The dependence of the droplet volume change on the maximum rms value of the acoustic velocity for methanol droplets with different initial diameters, calculated theoretically [using the correlations given by Eqs. (3b) and 10(b)], is shown in Fig. A1. Figure A1 shows that the droplet volume change is only a weak function of the initial droplet diameter. The droplet injection velocities were always less than 1 m/s. The theoretically computed droplet volume change for methanol droplets for different injection velocities calculated theoretically are plotted in Fig. A2, which shows that the results are nearly independent of injection velocity in this velocity range.

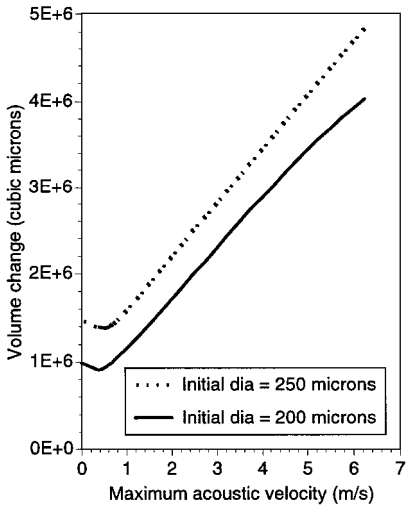

Fig. A1 Comparison of predicted volume changes of methanol droplets of different initial diameters moving a fixed distance along a standing wave as a function of acoustic velocity amplitude.

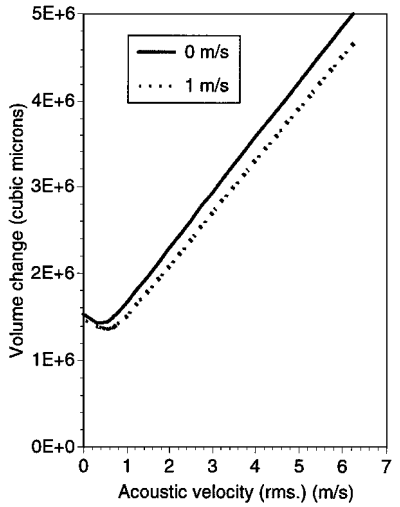

Fig. A2 Comparison of predicted volume changes of methanol droplets injected into the test section with different velocities moving a fixed distance along a standing wave as a function of acoustic velocity amplitude.

Acknowledgments

This work was supported by the Gas Research Institute under Contract 5089-260-1839. James Kezerle was the Contract Monitor.

References

[1] Bayley, F. J., Edwards, P. A., and Singh, P. P., "The Effect of Flow Pulsations on Heat Transfer by Forced Convection from a Flat Plate," *Proceedings of the International Heat Transfer Conference*, Vol. 59, 1961, pp. 499–509.

[2] Richardson, P. D., "Effects of Sound and Vibrations on Heat Transfer," *Applied Mechanics Reviews*, Vol. 20, No. 3, 1967, pp. 201–217.

[3] Al-Taweel, A. M., and Landau, J., "Mass Transfer Between Solid Spheres and Oscillating Fluids—A Critical Review," *Canadian Journal of Chemical Engineering*, Vol. 54, Dec. 1976, pp. 532–539.

[4] Lyman, F. A., "Attenuation of High-Intensity Sound in a Droplet Laden Gas," *Journal of Sound and Vibration*, Vol. 51, No. 2, 1977, pp. 219–235.

[5] Padmanabha, D., Nair, B. G., and Ramachandran, A., "Effect of Vertical Vibration on Mass Transfer from Spheres," *Indian Journal of Technology*, Vol. 8, July 1970, pp. 243–247.

[6] Sujith, R. I., Waldherr, G. A., Jagoda, J. I., and Zinn, B. T., "Experimental Investigation of the Behavior of Droplets in Axial Acoustic Fields," American Society of Mechanical Engineers Winter Annual Meeting, Chicago, IL, Nov. 1994; also *Journal of Vibration and Acoustics*, Vol. 119, No. 3, 1997, pp. 285–292.

[7] Sujith, R. I., Waldherr, G. A., Jagoda, J. I., and Zinn, B. T., "A Theoretical Investigation of the Behavior of Droplets in Axial Acoustic Fields," *Journal of Vibration and Acoustics*, Vol. 121, No. 3, 1999, pp. 286–294.

[8] Gemmen, R. S., Keller, J. O., and Arpaci, V. S., "Pulse Combustion: Numerical Analysis of Droplet Mass Transfer Enhancement, Thermo-Physical Aspects of Energy Conversion," ASME, Advanced Energy Systems, Vol. 16, 1990, pp. 81–90.

[9] Harpole, G. M., "Droplet Evaporation in High Temperature Environments," *Journal of Heat Transfer*, Vol. 103, 1981, pp. 86–91.

[10] Kouremenos, D. A., Rakopoulos, C. D., and Yfantis, E. A., "A FORTRAN Program for Calculating the Evaporation Rates in Diesel Engine Fuel Sprays," *Advances in Engineering Software*, Vol. 15, 1992, pp. 67–71.

[11] Drummond, C. K., "Numerical Analysis of Mass Transfer from a Sphere in an Oscillating Flow," Ph.D. Dissertation, Dept. of Mechanical Engineering, Syracuse Univ., Syracuse, NY, April 1981.

[12] Burdukov, A. P., and Nakoryakov, V. E., "On Mass Transfer in an Acoustic Field," *Journal of Applied Mechanics and Technical Physics*, Vol. 32, No. 2, 1965, pp. 51–55.

[13] Glassman, I., *Combustion*, Academic, New York, 1987, Chap. 6, Sec. 6, pp. 255–280.

[14] Clift, R., Grace, J. R., and Weber, M. E., *Bubbles, Drops and Particles*, Academic, New York, 1978, Chap. 11, pp. 285–320.

[15] Sujith, R. I., "Behavior of Droplets in Axial Acoustic Fields," Ph.D. Dissertation, Dept. of Aerospace Engineering, Georgia Inst. of Technology, Atlanta, GA, Nov. 1994.

[16] Odar, F., "Verification of the Proposed Equation for Calculation of the Forces on a Sphere Accelerating in a Viscous Fluid," *Journal of Fluid Mechanics*, Vol. 25, Pt. 3, 1966, pp. 591–592.

[17] Basset, A. B., *A Treatise on Hydrodynamics*, Vol. 2, Dover, New York, 1961, pp. 285–303.

[18] Landau, L. D., and Lifshitz, E. M., *Fluid Mechanics*, 2nd ed., Vol. 6, Course of Theoretical Physics, Pergamon, Oxford, England, UK, 1987, pp. 83–92.

[19] Press, W. H., Teukolsky, S. A., Vetterling, W. T., and Flannery, B. P., *Numerical Recipes*, 2nd ed., Cambridge Univ. Press, Cambridge, England,

UK, 1992, Chap. 16, pp. 701–740.

[20] Al-Taweel, A. M., and Carley, J. F., "Dynamics of Single Spheres in Pulsated, Flowing Liquids: Part I. Experimental Method and Results," *Proceedings of the Chemical Engineering Progress Symposium Series*, Vol. 67, No. 116, 1971, pp. 114–123.

[21] Baird, M. H. I., Senior, M. G., and Thompson, R. J., "Terminal Velocities of Spherical Particles in a Vertically Oscillating Liquid," *Chemical Engineering Science*, Vol. 22, No. 4, 1967, pp. 551–558.

[22] Herringe, R. A., "On the Motion of Small Spheres in Oscillating Liquids," *Chemical Engineering Journal*, Vol. 11, No. 2, 1976, pp. 89–99.

[23] Schoneborn, P. R., "The Interaction Between a Single Particle and an Oscillating Fluid," *International Journal of Multiphase Flow*, Vol. 2, 1975, pp. 307–317.

[24] Houghton, G., "The Behaviour of Particles in a Sinusoidal Velocity Field," *Proceedings of the Royal Society of London, Series A: Mathematical and Physical Sciences*, Vol. 272, 1963, pp. 33–43.

[25] Houghton, G., "Particle Trajectories and Terminal Velocities in Vertically Oscillating Fluids," *Canadian Journal of Chemical Engineering*, Vol. 44, April 1966, pp. 90–95.

[26] Zabrodskii, S. S., and Parnas, A. L., "Possible Intensification of Interface Heat and Mass Transfer in a Gas Suspension with Pulsating Resonance Flow," *Inzhenerno-Fizicheskii Zhurnal*, Vol. 9, No. 6, 1965, pp. 778–782.

[27] Drummond, C. K., "Mass Transfer from a Naphthalene Sphere Under Oscillatory Flow," M.S. Thesis, Mechanical Engineering Dept., Syracuse Univ., Syracuse, NY, 1979.